Analysis of Near-Capacity Iterative Decoding Schemes for Wireless Communication Using EXIT Charts

NASRU MINALLAH[1], MUHAMMAD FASIH UDDIN BUTT[2], (Member, IEEE),
IMRAN ULLAH KHAN[3], (Member, IEEE), ISHTIAQUE AHMED[4],
KHURRAM S. KHATTAK[1], GANG QIAO[3], (Member, IEEE),
AND SONGZUO LIU[3], (Member, IEEE)

[1]Department of Computer Systems Engineering, University of Engineering and Technology Peshawar, Peshawar 25000, Pakistan
[2]Department of Electrical and Computer Engineering, COMSATS University Islamabad, Islamabad 45550, Pakistan
[3]College of Underwater Acoustics Engineering, Harbin Engineering University, Harbin 150001, China
[4]National Center in Big Data and Cloud Computing, University of Engineering and Technology Peshawar (NCBC-UETP), Peshawar 25000, Pakistan

Corresponding author: Imran Ullah Khan (khan@hrbeu.edu.cn)

ABSTRACT This article proposes and compares the performance of three flexible and bandwidth efficient transceivers. The terminology of Over-Complete Mapping (OCM) is introduced in the first two schemes. All of the schemes, namely Non-Convergent Serial Concatenated OCM Coding (NCSCOC), Convergent Serial Concatenated OCM Coding (CSCOC) and Self-Concatenated Convolutional Coding (SECCC); are simulated for the Rayleigh channel and employing iterative decoding to attain the refined output stream for feeding the video decoder. Specifically, the iterative decoding is beneficial in acquiring the convergence of EXtrinsic Information Transfer (EXIT) curves by repeatedly sharing of the mutual information. The difference between the NCSCOC and CSCOC schemes lies in the inner and outer rates. This change reflects an improvement in the Bit-Error Rate (BER) and improved EXIT convergence of CSCOC scheme, with reference to NCSCOC scheme. Results show that NCSCOC scheme never reaches the point of perfect convergence despite iterative decoding. However, CSCOC and SECCC schemes succeed in securing perfect convergence. Investigating the BER curves, it is deducible that SECCC is the most desirable transceiver system, having the least BER. Furthermore, it is plausible that the overall performance of SECCC is much better than the preceding schemes. Explicitly, our experimental results show that the proposed CSCOC scheme outperforms its identical code rate counterpart NCSCOC scheme by about 3 dB at the Peak Signal-to-Noise Ratio (PSNR) degradation point of 1 dB. Additionally, an E_b/N_0 gain of 20 dB is attained using SECCC scheme relative to identical code rate NCSCOC benchmarked scheme.

INDEX TERMS Channel codes, concatenated codes, EXIT analysis, iterative decoding.

I. INTRODUCTION

Since the past few decades, wireless communication has revolutionized the outlook of fast and ubiquitous communication. Initially, wireless services were mostly used by the rich and some important security authorities, mainly due to the high power cost requirements. Researcher have put dedicated efforts to overcome the issue of power requirements while maintaining high data rate with a low error rate.

The associate editor coordinating the review of this manuscript and approving it for publication was Yougan Chen.

Explosive increase in the number of cellular mobile phones and the dramatic popularity of Internet has resulted in a challenge to maximize the achievable bandwidth accordingly [1], [2]. Next generation 5G communication aims at increasing the data rate manifolds in comparison with the 4G technology, by utilizing huge bandwidth available [3]. This escalation in the demand of wireless services is expected to grow continually, so researchers have to inevitably keep on designing efficient systems. Researchers believe that it is impractical to expect any fixed coding and modulation design that could best fit in a longer run [4].

In a broader context, codes are mainly classified as "Source Codes" and "Channel Codes". The sole purpose of source codes is to compress the data, whereas channel codes aim at transmitting data quickly over a coding scheme capable of correcting or at minimum detecting the errors. Moving from wireline to wireless communication, the inimical phenomenon of fading becomes prominent which is liable for unreliability in the latter. Transmission of a symbol over a non-ideal channel might put a contrary effect on the symbol as the received symbol is most likely to be different from the transmitted symbol. This difference in the received signal from the transmitted one arises because of the possible addition of channel noise [5]. The concept of redundancy and channel coding for a communication system is explained in detail in [6]. Redundancy is incorporated in channel coding to ensure that the original data is correctly destined [6] at the information sink. An innovative technique of artificial redundancy, known as Over-Complete Mapping (OCM) is explored in [7]. This article extends the work relating to OCM presented in our precursor conference paper [7], and then utilizes in two of the three developed channel coding schemes. Channel capacity is the ability at which any channel can reliably transmit information at the highest possible information rate. This paper carefully aims at contributing towards the design and analysis of new channel coding schemes for wireless communication.
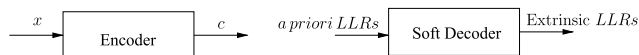

FIGURE 1. Block diagram of a simple encoder with its soft decoder.

A. BRIEF HISTORY AND PREVIOUS WORK

The advent of channel and hamming codes emanated in 1950s, advocating that the Bit-Error Rate (BER) performance of the signal is improved due to channel coding [8]. The higher data rate wireless communication requires higher bandwidth leading to higher BER as well. Therefore, employment of optimized channel coding techniques is the best possible solution to mitigate the BER without increasing the bandwidth [5]. The block diagram of a simple channel encoder accepting x as input for the output c, and its corresponding soft decoder [9] is depicted in Fig.1. The input *a priori* Logarithmic-Likelihood Ratios (LLRs) is transformed to *Extrinsic LLRs* after the decoding operation by the soft decoder. Error Correction can be divided into, Backward Error Correction (BEC) and Forward Error Correction (FEC) [10]. FEC coding is also known as channel coding. Claude Shannon, predicted that reliable transmission of bits can be accomplished with the aid of channel coding by introducing redundancy in the data bits, now known as Shannon Coding. Thanks to the breakthroughs in channel coding, it is feasible to design systems which are approaching Shannon's capacity and utilizing single transmitter and receiver [11]–[13]. Some important techniques of channel characterization, channel engineering and static transceiver

optimization are discussed in [14] for enhancing the wireless propagation scenario.

The proposition of turbo codes [15], envisaged the best since origination than any other class of codes because of its close Shannon-limit performance. Introduced by Berrou in 1993, they employ parallel concatenation of two Recursive Systematic Convolutional (RSC) codes incorporating an interleaver between the constituent encoders [16]. Consequently, remarkable gain in performance is observed with comparatively low complexity encoding and decoding algorithms. Discovery of concatenated coding scenario by Forney in 1965, is elaborated in [17]. In the early days, this family of codes was deprived of their due attention. But after the birth of turbo codes, concatenated coding started to grab its importance because of the fact that efficient iterative decoding was possible [4]. Concatenated codes are used to achieve lower BER with an overall little decoding complexity required than a single code of the same performance [18]. The advent of turbo codes has motivated numerous authors to expand the concept of iteratively decoded concatenated codes to other transmission schemes as well [19]–[21].

Concatenated coding scheme is divided into three main types, namely Parallel Concatenated Convolutional (PCC) codes, Self-concatenated Convolutional (ScC) codes and Serial Concatenated Convolutional (SCC) codes, depending on how the exchange of iterative information takes place among the constituent encoders [22]. In PCC coding, there are two or more constituent encoders combined in a parallel fashion. These constituent encoders may be a combination of RSC codes [16], Unity-Rate Codes (URCs) [23] or Trellis Coded Modulation (TCM) codes [24]; mutually sharing information via an interleaver. In ScC coding, the only component encoder is linked to an interleaver at the transmitter side, as shown in Fig.2. In SCC coding, M number of constituent encoders are concatenated serially with the help of $M - 1$ interleavers.
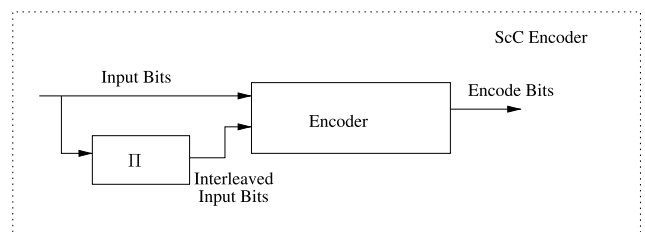
FIGURE 2. Block diagram of ScC encoder.

Extension of the concatenated coding to parallel scheme (turbo codes) is studied in [25]. Fig.3 and Fig.4 show the schematics of turbo encoder/decoder. The input u_1 and its interleaved version u_2 are fed to each encoder yielding the output c_1 and c_2 respectively which are processed by the MUltipleXer (MUX). Similarly for the turbo decoding, there are two decoders as well. The Demultiplexer (DEMUX) forwards the output stream to each decoder as *a priori* input. The extrinsic output from each decoder is interleaved,

FIGURE 3. Block diagram of turbo encoder.

FIGURE 4. Block diagram of turbo decoder.

deinterleaved and exchanged in a systematic manner with each other to generate the overall output. The notations A and E point the *a priori* and extrinsic data respectively.

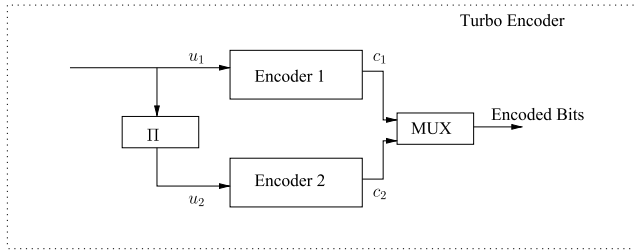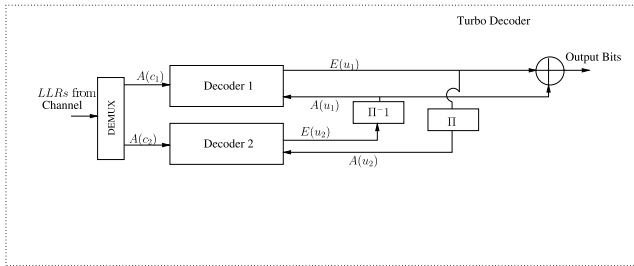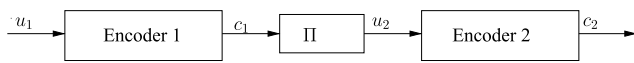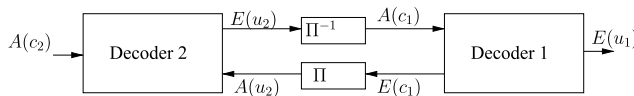**FIGURE 5.** Two-stage serial concatenated encoder.

FIGURE 6. Two-stage serial concatenated decoder.

Similarly, serial concatenation and the concatenated-convolutional linkage is done in [26]. The distinction between serial concatenated and parallel concatenated codes is that the information bits for the second code are not transmitted in turbo codes, hence increasing the code rate relatively to the serial one. The encoder structure is called parallel because both the encoders operate on the same set of input instead of one encoding the other output. Two-stage serial concatenated structure is demonstrated in Fig.5 and Fig.6. The input/output symbols and notations used are the same as discussed for the turbo case. Convolutional codes described in [27], are a powerful class of codes used in numerous systems of wireless standards as well as satellite communications. They are intuitive and there is always a way to decode and recover the mathematically most likely message from among the set of all possible ones. Different novel approaches for decoding the convolutional codes are presented in [28]–[31]. Convolutional codes are similar to the block codes in the sense that they utilize the transmission of parity bits that are computed from the message bits. However, they differ by not

sending the message bits followed by parity. In typical convolutional codes (other than systematic ones), only generated parity bits are send. For the systematic convolutional codes, information part is also transmitted along with the parity bits. Initially, Maximum Likelihood Sequence Estimation (MLSE) was deemed to be the most significant discovery for convolutional decoding in [32] and [33], until the dicovery of turbo codes. Maximum A Posteriori (MAP) decoding is somehow more complex than MLSE algorithm, but succeeds in lower BER for convolutional codes [34], is extensively finding applications after the discovery of turbo codes. One of the captivating reason for the large-scale deployment of convolutional coding in wireless communication is its ability to support soft-decision decoding. Block codes are capable of both hard-decision (0s and 1s) and soft-decision decoding. Several studies [35]–[37] recommend that there is a gain of 2-3 dB employing soft-decision over hard-decision decoding. Another attribute is the flexibility with which we can vary the code rate of convolutional codes using the concept of puncturing. For this, initially transmitter and receiver should agree on coded bits to omit, and then the puncturing table governs which bits to be included or discarded.

Differentiating turbo from convolutional coding, it is notable that turbo scheme produces randomness in coding due to the presence of an interleaver between the member encoders. Turbo codes are recursive, systematic, and with parallel structure. On the contrary, convolutional coding lacks interleaver, are non-recursive and non-systematic in operation.

Researchers have invested great efforts in optimizing the performance of concatenated codes for the improvement of BER curves and approaching near-capacity performance. Further improvement in BER is attained by invoking the iterative decoding processing [38], which together with the turbo principle [39] is put into service for parallel concatenated [15], [16], [25] and serial concatenated [26], [40], [41] codes. The technique of iterative decoding of serially concatenated codes was capitalized upon by numerous investigators [9], such as in turbo equalization, coded modulation, multi-user detection, joint channel-estimation and data-detection plus synchronization in addition to the concept of joint source-channel decoding [42].

B. OUR WORK
The next generation transceivers need to cope up with the escalating demands of higher performance efficiency operating nearest to capacity. With the above background, we have developed an arrangement of near-capacity channel coding schemes, namely Non-Convergent Serial Concatenated OCM Coding (NCSCOC), Convergent Serial Concatenated OCM Coding (CSCOC) and SElf-Concatenated Convolutional Coding (SECCC). The technique of OCM incorporates artificial redundancy to improve the performance of the iterative systems and is based on the property of open tunnel between the EXIT curves for achieving near-capacity operation. The schemes of NCSCOC and CSCOC are similar

in structure but differ only in the inner and outer code rates. Both schemes point to the employment of OCM as an outer code and RSC as an inner code. The unity-rate OCM in NCSCOC is specifically used to demonstrate the effect of parity bits on the overall BER and convergence behaviour of a scheme. The rate-4/9 OCM in CSCOC scheme generates artificial redundancy while in the case of unity-rate OCM of NCSCOC scheme, no redundancy is generated at all by the OCM encoder. To cope up with the requirement of consistent overall code rate, the inner encoder rate is accordingly managed in both the schemes. With this mere alteration in the outer and inner rates, the CSCOC scheme becomes much more beneficial than the NCSCOC scheme in terms of BER and the convergence behaviour. For the SECCC scheme, an employment of single RSC as an inner encoder is discussed with the concept of puncturing. The single encoder SECCC scheme offers a very simpler approach but avoids any compromise on performance. The puncturing and RSC rates are set accordingly to strive for the best possible BER performance and EXtrinsic Information Transfer (EXIT) convergence of the SECCC scheme. In short, all the schemes are simulated for a consistent overall code rate. We will be deploying iterative decoding in all schemes for the sole purpose of low BER. The three schemes are subjected to BER, Peak Signal-to-Noise Ratio (PSNR) and EXIT charts investigations for their performance metrics.

To be more precise, the contribution of this research work includes:

- Introduction to the concept of OCM and its beneficial combination with RSC to achieve iterative convergence.
- Introduction to SECCC scheme and its performance comparison with NCSCOC and CSCOC schemes.
- Relative convergence behaviour analysis of SECCC, CSCOC and NCSCOC schemes using EXIT charts.
- The performance analysis of high compression efficient H.264/Advanced Video Coding (AVC) standard, using the schemes of SECCC, CSCOC and NCSCOC to provide insight into the performance of video streaming for the proposed schemes.

The rest of the article is structured as follows. In the subsections of Section II, the proposed schemes are fully covered. Section III highlights the important terminologies related to the schemes presented in the treatise. Section IV is about EXIT analysis, followed by some applications of EXIT charts. Results are presented and discussed in Section V. In Section VI, the conclusion is declared with some future research work description.

II. PROPOSED SCHEMES

The proposed channel coding schemes are simulated using the signal processing and communication library of C++, namely IT++. Furthermore, in order to have similar computational complexity of the presented iterative schemes, a consistent number of 26 iterations is set for each scheme to obtain their respective results of BER, PSNR and EXIT curves.

The working of proposed near-capacity iterative decoding schemes is individually elaborated in the subsections to follow. In each scheme, the inner encoder is recursive in structure as it augments the interleaver gain and sidesteps the formation of a BER floor in an iterative decoding scenario [40], facilitating the inner EXIT curve to reach the point of convergence. This article presents a novel combination of the OCM-RSC in a favourable and advantageous way for the incorporation of redundancy in proposed channel coding schemes. This OCM-RSC combination offers flexibility with which we can easily control the redundant bits in our bandwidth efficient channel coding designs, operating close to capacity. OCM caters for the artificial redundancy and enhances the performance by increasing the reliability of schemes. Puncturer of a specific rate is employed to stop the transmission of certain number of encoded bits. URCs are specifically helpful in achieving low-complexity designs for efficient systems with stringent BER requirements and iterative detection [4].

The design of OCM is based on a specific property of EXIT charts, that is the iterative decoding system is capable of near-capacity operation only if there is an open tunnel between the constituent EXIT curves. This open tunnel results in the intersection of curves at (1, 1) point of convergence. For this criterion to be met, Kliewer *et al.* [43] suggested that the minimum Hamming distance of $d_{H,min} = 2$ must be fulfilled for all the legitimate codewords. OCM operation is demonstrated with the help of TABLE 1. Rate-1 OCM adds no parity bit while rate-3/4 OCM augments a single parity for 3-*bit* symbols, such that even parity is followed by all the resulting 4-*bit* symbols. It can be seen that the condition of $d_{H,min} = 2$ is satisfied. It is worth mentioning that only eight out of the sixteen possible 4-*bit* symbols are valid. The performance of Soft-Bit Source Decoder (SBSD) greatly depends on the presence or absence of such redundancy, as demonstrated in Section V.

TABLE 1. Symbols representation with rate-1 and rate-3/4 OCM.

Symbols	Rate-1 OCM	Rate-3/4 OCM
000	000	0000
001	001	1001
010	010	1010
011	011	0011
100	100	1100
101	101	0101
110	110	0110
111	111	1111

ScC is similar to PCCC when the two component codes in PCCC are replaced by one component code (having hypothetical upper and lower component encoders) with the aid of an odd-even separated turbo interleaver, as discovered in [44]. This results in a less complex turbo encoder design. The SECCC decoder works by iteratively exchanging extrinsic

information (self-iterations) by the component code with the aid of an interleaver pair as seen in Fig. 10. The soft extrinsic information of the decoder is used for the next decoding as its *a priori* input which improves its knowledge and hence performance.

A. NON-CONVERGENT SERIAL CONCATENATED OCM CODING (NCSCOC)

The block diagram of our proposed NCSCOC scheme is shown in Fig. 7. In the modern era, video transmission is assisted by any of the video compression standards. In this treatise, we consider the H.264 standard (also known as AVC codec), for video encoding and decoding in all of the schemes. H.264 was designed to meet the fast and next-generation communication requirements, significantly outplayed all the previous standards via its complicated and efficient techniques [45]. The beauty of this standard is that some of its features are retained in the latest evolving standard H.265 [46], making it still a fascinating standard for researchers.
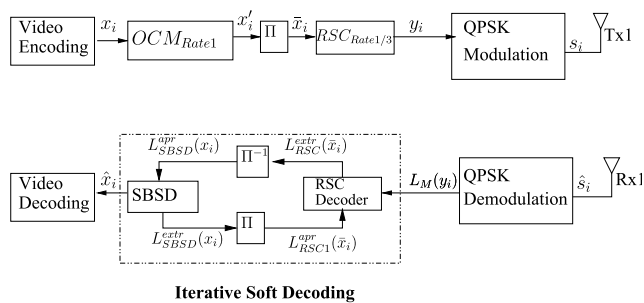

FIGURE 7. Block diagram of NCSCOC scheme.

After video compression at the video encoder, this scheme employs OCM as an outer code of unity-rate, RSC encoder with a 1/3 rate as the inner code and the modulation technique of Quadrature Phase Shift keying (QPSK). The overall code rate is simply the multiplication of inner and outer code rates. It is worth mentioning that the video compression operation retards the overall performance at the receiver. The limited performance phenomenon is owing to the inherent residual limited redundancy in the AVC codec. So in order to rectify this situation, the novel technique of OCM is greatly beneficial. OCM generates artificial redundancy [7] in the encoded stream to recover the information more reliably at the receiver. It is worth mentioning that rate-1 OCM results in no addition of redundancy in the original bit-stream. As stated in Section II above, the unity-rate OCM adds no parity bits and hence no artificial redundancy in the coded bit-stream. Furthermore, it can be seen from TABLE 1 that the convergence condition of $d_{H,min} = 2$ is not satisfied by the unity-rate OCM and hence the outer OCM code might not be capable to reach the point of perfect convergence. The bit-stream x_i is converted to bit-string x_i' after the outer OCM operation. Here, the range of bits in a bit-stream is specified as $i = 1, 2, 3 \ldots n$, where n is the total number of bits

and the whole process is repeated for each and every bit. In order to mitigate the effects of burst of errors, bit string x_i' is passed through an interleaver (Π), resulting into $\bar{x}_i$. Interleaving renders the bursty error data capable of being corrected by the error correcting codes. According to [47], the length of an interleaver is directly associated with the degree of statistical independence arising in the data. So the interleaver spreads the bursty error data and makes it independent, achieving correctability. The only downside of employing higher interleaving is the delay in the encoded video sequence. As we have utilized the H.264/AVC standard codec sequence in Quarter Common Intermediate Format (QCIF) with (176 × 144)-pixels or 99 Macro-Blocks (MBs) each of size (16 × 16)-pixels. Therefore, in order to augment the interleaver length without any delay, the technique of concatenated 99 Macro-Blocks (MBs) per frame is utilized, improving the efficiency of iterative decoding as well. In the next stage, $\bar{x}_i$ is forwarded to the RSC encoder via an appropriate Generator Polynomial (GP). The octal format GP of RSC encoder used is $(G_0, G_1, G_2 = 13, 15, 17)$. The RSC encodes the $\bar{x}_i$ sequence into y_i, which is mapped by the QPSK modulator into a sequence s_i, where $i = 0, 1, 2, 3 \ldots l - 1$, and l represents the modulated symbols. Eventually, the symbols are transmitted via transmitter Tx1.

On the receiver side, receiving antenna Rx1 receives the signal and decoding is initiated with the QPSK demodulation, followed by iterative soft decoding due to its prolific gain. The demodulated signal is fed to the RSC decoder, yielding the logarithmic extrinsic information $L_{RSC}^{extr}(\bar{x})$ which is deinterleaved (Π^{-1}) to serve as the *a priori* input to the SBSD. SBSD outputs $L_{SBSD}^{extr}(x)$ which may be served as an *a priori* input after interleaving to the RSC. Accordingly, the outer and inner decoders share sufficient LLR values in each iteration using the concept of interlacing. This iterative process continues until an approximate signal $\hat{x}_i$ is received. After the iterative soft decoding process, the bit-stream is fed to the standard video decoder for generating the output video.

B. CONVERGENT SERIAL CONCATENATED OCM CODING (CSCOC)

In CSCOC scheme, we have merely changed the rates of inner and outer codes from that presented in NCSCOC. In this scheme we employ rate-3/4 OCM as an outer code and RSC encoder with a 4/9 rate as the inner code, while keeping the overall code rate identical to that of NCSCOC scheme. As stated in Section II, the rate-3/4 OCM adds a single parity bit to the 3-bit symbol and hence artificial redundancy is introduced in the coded stream. Furthermore, it can be seen from TABLE 1 that the convergence condition of $d_{H,min} = 2$ is satisfied by the rate-3/4 OCM and hence the outer OCM code might be capable to reach the point of perfect convergence. With the use of rate-3/4 OCM as an outer code, we will show with the aid of EXIT chart that how this artificial redundancy affects the convergence behaviour of CSCOC scheme. The octal format GP of RSC encoder used

is $(G_0, G_1, G_2 = 13, 15, 17)$. All the other settings (including the overall code rate) remain the same as shown in Fig.8. The effects of this alteration in inner and outer rates is discussed in Section V.
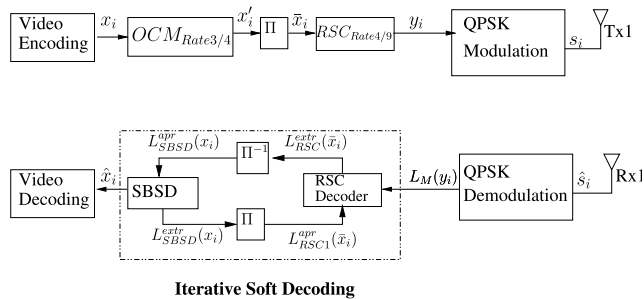

FIGURE 8. Block diagram of CSCOC scheme.

C. SELF-CONCATENATED CONVOLUTIONAL CODING (SECCC)

Based on the concept of ScC codes given in Section I, we present our design of SECCC with iterative decoding. The schematic diagram of our SECCC scheme is depicted in Fig. 9. The special feature about the SECCC scheme is its single encoder (little complexity). Video encoded bit-stream is passed to the SECCC encoder before it is QPSK modulated and allowed to propel over a Rayleigh channel. At the receiving terminal, we have a SECCC decoder taking samples from the QPSK demodulator and forwarding to the video decoder. The SECCC encoder/decoder structure is explicated below.
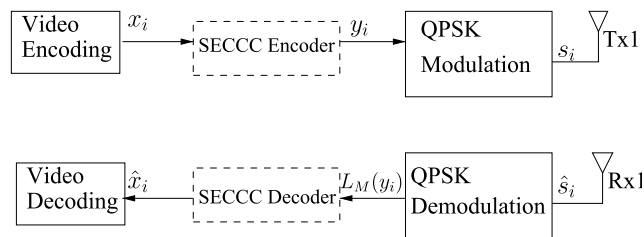

FIGURE 9. Block diagram of SECCC scheme.

Loeliger was the pioneer of the concept of self-concatenated coding after great inspiration by the turbo codes. A self-concatenated code with an interleaver is a scheme based on only one RSC encoder, simplifying the process but ensuring no compromise on performance. These low-complexity codes are best suitable for the construction of trellis coded modulation, based on one trellis [22]. The bit-error probability of all the related interleavers is governed by the maximum-likelihood decoding.

Fig. 10 explains visually the overall two-stage SECCC structure. The term "Two-stage" refers to the stages of two main components, namely "RSC Encoder" and "Puncturer" of the SECCC structure. The two major components are separated with the help of an interleaver, for the sake of randomness in the coded bits before the puncturer and distinguishing the two-stages more clearly. The information or data

bits d_k from source encoder (H.264/AVC) and its interleaved version d_k' are simultaneously fed to the Parallel-to-Serial (P/S) converter, and forwarded to the RSC encoder of rate R_1 and memory v via an appropriate GP. The octal format GP used in our design is $(G_0, G_1, G_2 = 13, 15, 17)$. Afterwards, puncturing at the rate R_2 is carried, which stops some bits from transmission, for enhancing the bandwidth efficiency. For a rate 3/4 puncturer, one bit out of four encoded bits gets punctured. So at the output of puncturer, the number of bits get reduced from the number of bits which were increased as a result of R_1. It is worth mentioning that the bits which may get stopped by the puncturer, could potentially be either the systematic or parity bit. The overall code rate R is as given in [10]. These bits are then QPSK modulated, resulting in symbols via the technique of Gray-Mapping (GM). Finally, transmission of these symbols is carried over the channel.
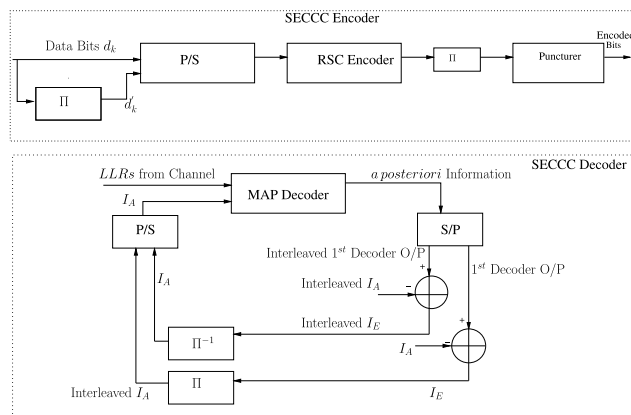

FIGURE 10. Two-stage SECCC structure.

The interleaver placed before the P/S converter in Fig. 10 renders the information bits highly uncorrelated, necessary for the Gaussian distribution of information bits to be efficiently employed in EXIT charts. The interleaver used after the RSC encoder is meant to randomize the encoded bits before the puncturer, distinguishing the two stages of SECCC as well.

$$R = \frac{R_1}{2 \times R_2} \qquad (1)$$

Changing the values of R_1 and R_2 provides the flexibility of designing various codes. At the receiver side, SECCC decoder takes logarithmic decoded symbols. For this, the received demodulated symbols may be led to the demapper for the calculation of conditional Probability Density Function (PDF). Here the SECCC decoder services by set number of self iterations only. Resulting PDFs are then passed to a soft-depuncturer, converting them to LLRs and adding zeros in place of missing LLR values, incurring for the concept of puncturing as discussed in [10]. These LLRs are given at the input of Soft-Input-Soft-Output (SISO) MAP decoder, yielding *a posteriori* information, favourable in the generation of EXIT curves. The functionality of MAP decoder is exquisitely explained in [24]. The *a posteriori* information

is modified via Serial-to-Parallel (S/P) converter, resulting in the 1st decoded Output (O/P), interleaving which yields the interleaved version of output. In an appropriate interleaving/deinterleaving of the information bits as discussed in [10], *a prior* LLRs are generated. All of this decoding process is based on a fixed number of iterations. The same process is repeated several times and information is continuously shared to the constituent MAP decoder, as well as between the decoder and soft-demapper, until the desired decoded bits yield [10]. This self-iteration services in the improvement of coding scheme. The decoded stream is ultimately supplied to the standard video decoder for the end users' experience.

The parametric comparison among the three schemes is depicted in TABLE 2.

TABLE 2. Comparison of the proposed channel coding schemes.

Scheme	Bit Rate			Modulation
	Inner Code	Outer Code	Overall Code Rate	
NCSCOC	Rate-1/3 RSC	Rate-1 OCM	1/3	QPSK
CSCOC	Rate-4/9 RSC	Rate-3/4 OCM	1/3	QPSK
SECCC	R_1=1/2 RSC	R_2=3/4 Puncturer	1/3	QPSK

III. PARAMETRIC TERMINOLOGIES USED IN THE SCHEMES

Interleavers are used between the constituent encoders of serial or parallel structures to introduce time diversity and to reduce the correlations in the data exchanged between the decoders, providing independent extrinsic information. Furthermore, interleavers effectively transform a bursty channel into a random channel by spreading a burst of errors across the whole decoded frame. The length of interleaver is an important parameter in determining the code's distance properties. The objective of an interleaver is to improve the distance properties of the corresponding code. Conclusively, interleaver design significantly affects both the BER "turbo cliff" and the "error floor". Longer interleaver tends to give more Gaussian-like LLR distributions, resulting in a system's BER performance approaching to Shannon's capacity limit.

For the constituent decoders process, Robertson introduced the concept of **LLR**, which is extensively utilized in iterative decoding schemes. The LLR is equivalent by definition as in [9]

$$L(b_k) \triangleq \ln(\frac{P(u_k = +1)}{P(u_k = -1)}) \qquad (2)$$

$L(b_k)$ represents the LLR of bit b_k, which is the logarithm of the ratio of probability of the bit b_k taking on its two admissible values. $P(u_k)$ symbolizes the probability of bit u_k, correspondingly for values +1 and −1.

Some of the other decoding specific terms are:

- *a priori* **Information** It is the known information about a bit even before the start of decoding process, also known as intrinsic information and denoted by I_A.
- *a posterior* **LLR** The output of the member decoder accepting channel and *a priori* LLRs is known as *a posteriori* LLR.

- **Extrinsic Information** Subtracting the *a priori* information from the output of the first member decoder results in Extrinsic Information (I_E). Interleaving/de-interleaving makes I_E to serve as *a priori* information for the other constituents.

IV. EXIT CHART ANALYSIS

After the valuable contribution of iteratively decoded systems in various transmission schemes, the primary centre of attention was to devise tools for evaluating their convergence behaviour [48]–[51]. Stephen ten Brink proposed the employment of EXIT characteristics by examining the flow of input/output mutual information exchange between the component SISO decoders [52]. EXIT chart analysis serves as a powerful tool to predict the convergence behaviour of systems involving iterative exchange of information between the essential components [38], [53]–[56]. The main advantage associated with EXIT chart analysis is the ease with which it offers fast approach to predict convergence at infinitesimal BER values, avoiding the time consuming Monte-Carlo simulations for BER predictions [57]. Mutual Information (MI) gives the basis to the concept of EXIT charts [9], [53]. The curves on the EXIT chart represent the constituent decoders of a scheme. An EXIT curve is based on the corresponding MI resulting from I_A and I_E. Mathematically, Information (I) is defined by (3). If a source is producing "q" equi-probable levels, with the probability $p_i = 1/q$, where $i = 1, ..., q$, then I carried by each level is

$$I = \log_2(\frac{1}{p_i}) = \log_2(q) \qquad (3)$$

For average I [9], it is useful to define entropy H (in bits) as in in (4).

$$H = \sum_{i=1}^{q} p_i I_i \qquad (4)$$

Specifically, the EXIT chart analysis aims to compute the MI $I(X; L)$ in iteratively decoded schemes between the transmitted systematic bits X and L, where L represents the LLRs of bits [49], [53]. If the value of $I(X; L)$ continues to grow (till 1) during the iterative process, the decoding is considered to be good and successful. Increasing I_A shows that the more bits become known at the component decoder, providing a higher I_E value as well. The information contents of I_A and I_E are computed in a similar fashion. The range of values applicable to both I_A and I_E is given by (5) and (6) respectively. The detailed EXIT chart analysis is presented in [49]. Different values of E_b/N_0 result in different EXIT curves. The relation between I_E and I_A for various values of E_b/N_0 is elaborated in [49], given as in (7).

$$0 \leq I_A \leq 1 \qquad (5)$$
$$0 \leq I_E \leq 1 \qquad (6)$$
$$I_E = T(I_A, E_b/N_0) \qquad (7)$$

Here T represents the transfer characteristics function, inverse of which also exists on

$$T(0) \leq I_E \leq T(1) \qquad (8)$$

EXIT charts operate on the assumption of employing high interleaver lengths so that the *a priori* LLRs becomes uncorrelated and Gaussian distributed [4]. Instead of performing the prolonged bit-by-bit decoding simulations, EXIT charts offer a handy approach to quickly predict the Signal-to-Noise Ratio (SNR) value where an extremely low BER can be achieved [58].

Authors in [9] describe as predicting the convergence behaviour of the iterative decoders is the main purpose of employing EXIT charts. These charts find functionality in serial concatenated systems, parallel concatenated systems and hybrid systems as well. EXIT charts provide with a useful and quick technique of designing near-capacity systems [4]. Besides this, EXIT chart can be utilized in estimating the channel capacity and the code rate [55]. Ideally, the EXIT curves should converge at the E_b/N_0 value of interest after the exchange of extrinsic information by intersecting at the (1, 1) point. This perfect convergence condition gives appearance to a so-called *convergence tunnel* on the EXIT chart. In some cases, *semi-convergent tunnels* are also recorded which indicate that a moderately low BER can be achieved, albeit it will be higher than the infinitesimal BER achieved as a result of perfect convergence. It is reported that the obtained EXIT chart tunnel is always wider than the predicted one. According to [4], more iterations are needed to reach the (1, 1) point of convergence as the *convergence tunnel* becomes narrower, resulting in a performance closer to the channel capacity. As regards the convergence performance, the wider the *tunnel* the better and the value of I_E should closely be near to 1 [54]. The EXIT chart results may be verified by the Monte-Carlo simulation based iterative decoding trajectory.

Taking interleaving into consideration, the system with a shorter depth of interleaver will need more iterations to reach the highest intersection point between the EXIT curves of the inner and outer decoders [9]. As reported in [9], increasing the interleaving bits from 10^3 to 10^4 bits, a significant improvement in BER performance is observed. Paradoxically, increasing the interleaving bits from 10^4 to 10^5 bits, a very slight improvement is recorded, while any further increase fails to offer considerable improvement in the BER of a system.

A. APPLICATIONS OF EXIT CHARTS
Some applications pertaining to the EXIT charts which are extensively elaborated in [9] are as:
- Fruitful in developing code design and setting a trade-off between design criteria for developing good codes, having the maximum possible effective free distance.
- EXIT charts are helpful in choosing the best arrangement of the constellation mapping together with the inner and outer code GPs.

- Irregular codes can be designed easily using EXIT charts.
- Offers much simpler approach to various techniques of coded modulation.
- Helpful in the development of EXIT band charts.

V. SIMULATION RESULTS
In this section we present our simulations results characterizing the proposed systems work. In our simulations, we have exerted a 45-frame *Akiyo* video sequence characterized by QCIF in (176 × 144)-pixels. The video encoding is done via the H.264/AVC Joint test Model (JM) 19.0 reference codec operating at 15 frames-per-second (*fps*) and 64 *kbps* bitrate. Each QCIF frame is subdivided into 9 slices, each slice possessing 11 MBs. In the interest of reduced error propagation, each intra-coded '*I*' frame at 15 *fps* is accompanied after by 44 predicted '*P*' frames, such that a time lag of 3 seconds exists between two consecutive '*I*' frames. Besides this, we subsumed the technique of intra-frame coded MB updates of three arbitrarily distributed MBs per frame, in order to further minimize the effects of error propagation. Keeping the complexity of the video coding scenario to be least, the technique of multiple reference frames for inter-frame motion was not availed. To subsist on the motion search, we used barely the immediately preceding frame, providing a much lower computational complexity in comparison to multiple reference frames.

The final source coded stream is fed to the proposed schemes for channel coding and transmitted to the receiver side. Setting the overall code rate equal for all the schemes and other parameters as specified in TABLE 2, paves the path for our analysis. In order to increase the confidence in our simulations, we have used a consistent number of 10^4 interleaving bits, 10 transmission frames and 20×10^3 information bits in all of the proposed schemes. A consistent number of 26 iterations is set for each scheme to obtain the results of BER, PSNR and EXIT curves. For further increasing the confidence in our results, we repeated each 45-frame experiment 250 times and averaged the generated results.

BER, code rate, code gain, coding and interleaving delay, system bandwidth, effective throughput and channel characteristics are deemed to be important factors that affect the design of channel coding and modulation schemes as pointed out in [2]. BER is a term widely used in telecommunication and is meant for the indication of how frequently or at what pace the transmitted packet of bits needs to be retransmitted due to occurrence of an error in the received bits, commonly expressed in negative powers of ten. As a general aim, researchers strive for achieving lower BER as possible without affecting the intended communication.

Inspection of Fig.11 reveals that the SECCC scheme is significantly better in BER performance during most of the interval span in comparison with the NCSCOC and CSCOC schemes. The BER curve of SECCC scheme approaches to 10^{-5} (negligible value) within the least time in comparison
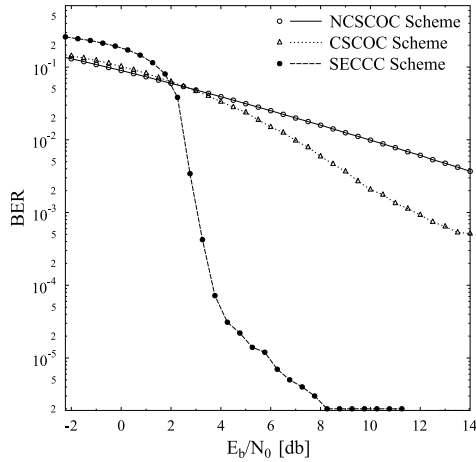
FIGURE 11. BER comparison of the proposed schemes.

FIGURE 12. PSNR comparison of the proposed schemes.

with the other schemes. So we infer that SECCC is a convincing system for achieving lower BER with more bandwidth efficiency. For the CSCOC, a mere change in the outer and inner rates from that used in the NCSCOC, leads to considerable improvement in BER. Technically, this improvement in BER performance is governed by the rate-4/9 OCM which generates artificial redundancy in the CSCOC scheme. Furthermore, the generated artificial redundancy is responsible for EXIT convergence of the CSCOC scheme for a range of E_b/N_0 values, by yielding an open tunnel between the constituent EXIT curves for achieving near-capacity performance. Having said that CSCOC is better that NCSCOC on account of BER, it is clear from Fig.11 that SECCC surpasses the other schemes. More specifically, it is observed that the proposed CSCOC scheme with convergence capability outperforms its non-convergent counterpart NCSCOC scheme by about 4.5 dB E_b/N_0 at the BER degradation point of 5×10^{-3}. Furthermore, an E_b/N_0 gain of 5 dB is attained using iterative SECCC scheme capable to reach the point of perfect convergence, with reference to CSCOC scheme. Additionally, an E_b/N_0 gain of 8.5 dB is attained using iterative SECCC scheme, with reference to NCSCOC scheme. So the BER measured performance favours the SECCC scheme.

PSNR is a term widely used to measure the visual quality of an image or video signal by determining the ratio between the original signal and the noise. It is usually calculated in the logarithmic (dB) scale to measure the quality of any reconstructed signal with respect to its reference or ground-truth signal. The greatest advantage of PSNR is the ease and simplicity with which it can be computed from the Mean Squared Error (MSE) between the original and reconstructed image or video sequence pixels [59]. PSNR uses MSE term in the denominator, so there is an inverse relation between them. The PSNR is reported to assess the perceptual quality well when fixed content and codec is carried across all the cases [59]. The performance trends of our proposed schemes expressed in terms of the PSNR versus E_b/N_0 are depicted in Fig.12. It can be seen in Fig.12 that the SECCC scheme
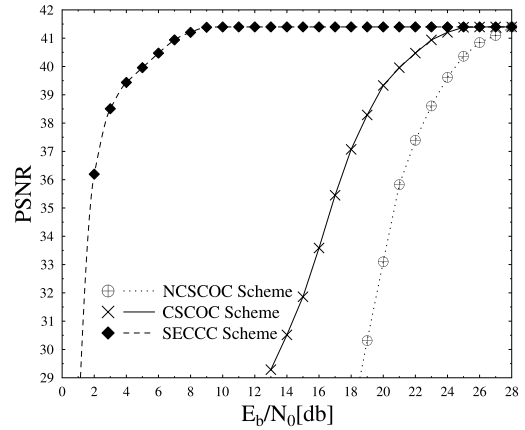
offers the best PSNR performance among the three different schemes of TABLE 2 across the entire range of E_b/N_0 considered. It is also derivable from Fig.12 that upon using unity-rate outer OCM in conjunction with the rate-1/3 inner RSC of NCSCOC scheme, results in an unsatisfactory PSNR performance than the case of rate-3/4 outer OCM combined with the rate-4/9 inner RSC of CSCOC scheme. Quantitatively, using the SECCC scheme of TABLE 2, an additional E_b/N_0 gain of upto 20 dB is attained over the identical rate NCSCOC benchmarked scheme. Thus, SECCC is the best PSNR performance offering scheme.

Moving to the third performance indicator, we evaluate the convergence behaviour of our schemes. EXIT Chart analysis is a very useful technique in analyzing the convergence behaviour of iteratively decoded schemes. Specifically, such an analysis becomes beneficial for the iterative schemes because of the fact that BER offers bad performance in regions of low E_b/N_0 and turbo cliff. In such cases, EXIT charts accurately estimate the BER performance [60]. Though Fig.11 appeals in support of an argument for the deployment of SECCC, yet it will be interesting to visualize the EXIT curves for the presented schemes.

Fig.13 portrays the EXIT curves of the NCSCOC scheme for the set overall code rate of 1/3 and operating in the $E_b/N_0 = [2, 11]$ dB range from downward to upward curves with steps of 1 dB each. It is easy to figure out that the NCSCOC scheme never converges, as the curves never meet the $(1, 1)$ point on the graph. It can be inferred that rate-1 OCM is not good enough to exploit the advantage of iterative decoding. It is plausible that the EXIT curves of NCSCOC scheme never reaches to $(1, 1)$ point of convergence. This puts a severe setback for the NCSCOC scheme.

For the CSCOC scheme, EXIT curves of Fig.14 show that this scheme achieves the perfect convergence point $(1, 1)$ for different values of E_b/N_0. The CSCOC scheme is operating in the $E_b/N_0 = [2, 16]$ dB range from downward to upward curves with steps of 1 dB each. So we deduce that employment of inner rate-4/9 RSC and outer rate-3/4 OCM, offers much fruitful result as iterative decoding becomes more favourable for sharing of mutual information between the
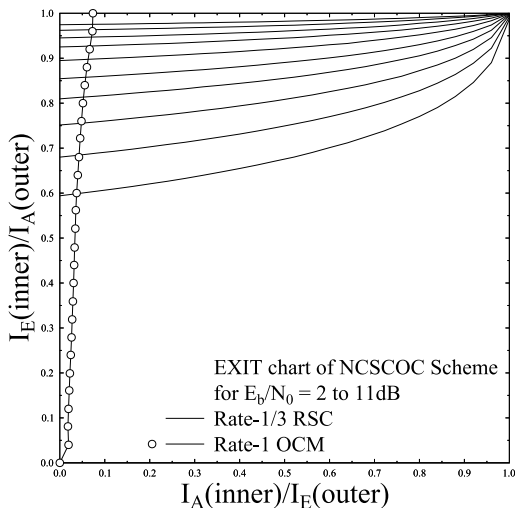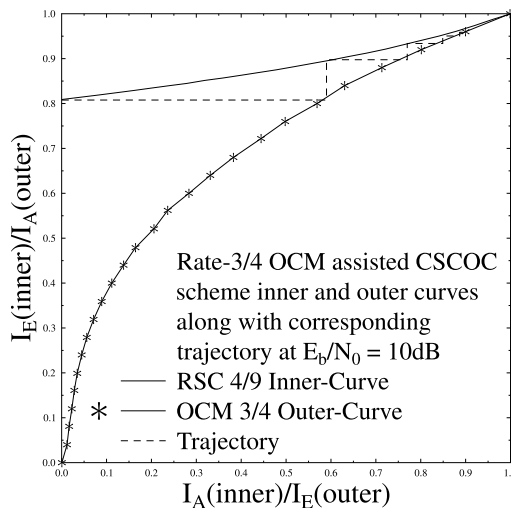
FIGURE 13. EXIT curves of NCSCOC scheme operating in the $E_b/N_0 = [2, 11]$ dB range from downward to upward curves with steps of 1 dB each.
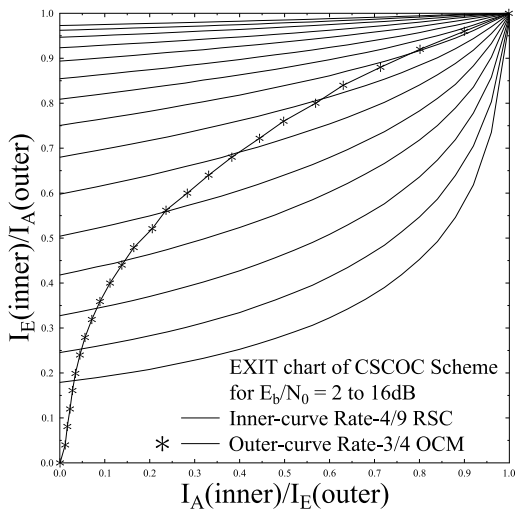
FIGURE 14. EXIT curves of CSCOC scheme operating in the $E_b/N_0 = [2, 16]$ dB range from downward to upward curves with steps of 1 dB each.

FIGURE 15. EXIT curves of CSCOC scheme at $E_b/N_0 = 10$ dB.

the help of 10^5 information bits is shown with the dotted line style to reach the point of convergence, after iterating between the inner and outer EXIT curves.

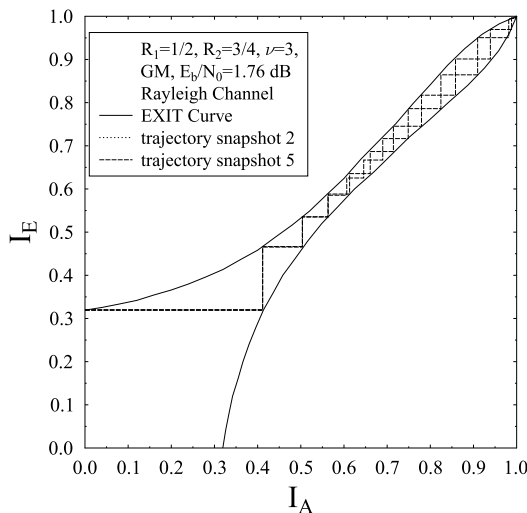**FIGURE 16.** EXIT curves of SECCC scheme at $E_b/N_0 = 1.76$ dB.

component decoders, leading to perfect convergence. It is inferable from the EXIT curves of NCSCOC and CSCOC schemes that a mere change in the outer and inner rates, significantly affects the convergence behaviour, keeping the overall code rate and component encoders constant. In fact, the artificial redundancy of single bit introduced by the rate-3/4 OCM code is responsible for the convergence of EXIT curves.

After the EXIT chart curves of CSCOC scheme in Fig.14, it will be useful to know the trajectory of the CSCOC scheme. As shown that the CSCOC scheme converges for a variety of E_b/N_0 values for, it is highly anticipated that the trajectory curve for the said scheme would also reach the (1, 1) point of convergence after iterating between the constituent EXIT curves. This is validated by the EXIT chart of Fig.15 at an E_b/N_0 value of 10 dB. The obtained trajectory curve with

In Fig.16 to Fig.18, the two EXIT curves for the SECCC scheme which are shown to be identical (mirror of each other) along the 45 degree diagonal line, are plotted with the solid line style. The two Monte-Carlo simulation based trajectories are plotted in Fig.16 and Fig.17, which correspond to the iterations in between the two EXIT curves. Each decoding trajectory snapshot is computed with the help of 10^5 information bits. For the sake of clarity, one snapshot is potted with the dotted line and other with the dashed line style. The snapshots are samples of trajectories which we average to obtain the overall trajectory. In our simulations, we have used a total of 10 snapshots to obtain the averaged sample. The two snapshots (each with a number) in each Fig.16 and Fig.17 are randomly chosen and plotted to show two samples of trajectories for the SECCC scheme. In Fig.18, the averaged
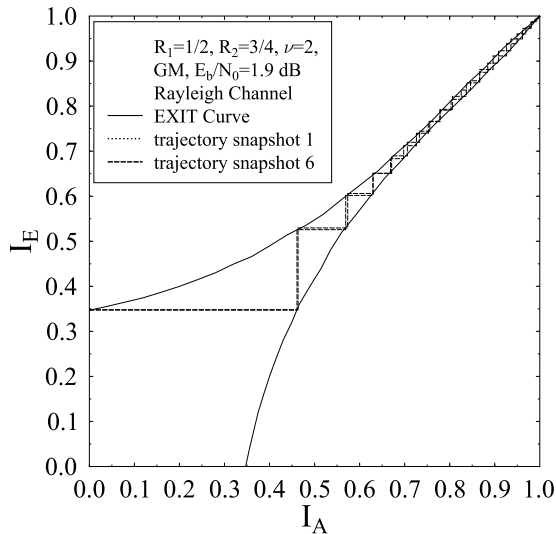
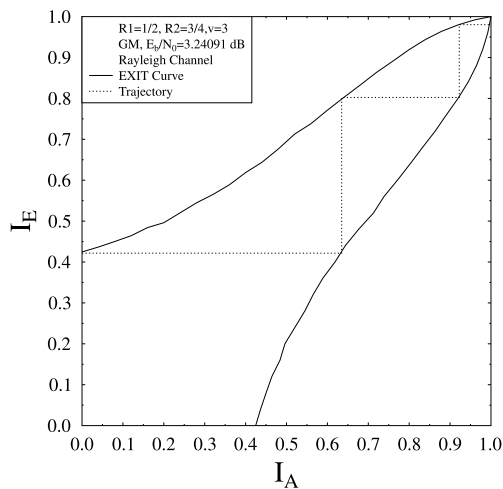**FIGURE 17.** EXIT curves of SECCC scheme at E_b/N_0 = 1.9 dB.

FIGURE 18. EXIT curves of SECCC scheme at E_b/N_0 = 3.24091 dB.

overall trajectory is plotted with the dotted line style, iterating between the corresponding EXIT curves.

For the SECCC scheme, deployment of the overall rate of 1/3 with a code memory of 3, yields the curves as in Fig.16. The stair-shaped trajectories which are arbitrarily selected and plotted alongside the EXIT curves, represent the Monte-Carlo simulation based iterating trajectories. The two EXIT curves of SECCC are always identical with reference to the diagonal line, since they refer the identical decoder. It is clearly seen that at even a comparatively lower E_b/N_0 value, the SECCC scheme ultimately reaches a (1, 1) point of convergence. Further, with the increase in E_b/N_0 value and reduction of memory to 2, still the point of convergence is achieved as shown in Fig.17. In a similar increasing fashion of E_b/N_0, we visualize a wide open tunnel in the EXIT chart of Fig.18. It is deducible that considerable increase in E_b/N_0 value results in fewer iterations to convergence as in Fig.18. This confirms the claim that more number of iterations are required to reach convergence as the *convergence tunnel* becomes narrower. Convergence is achieved in the CSCOC

scheme. However, the convergence tunnel of SECCC scheme at lower E_b/N_0 values of 1.76 dB and 1.9 dB is very much narrower and reaches precisely to the point of perfect convergence. In comparison with SECCC, the CSCOC scheme requires very high E_b/N_0 value to reach to the point of perfect convergence. It can be observed from Fig.15 that, although the CSCOC scheme is capable to gain iterative gain but its EXIT tunnel is unable to iteratively reach the point of perfect convergence at considerable higher E_b/N_0 value of 10 dB as shown in Fig.15. Furthermore, the CSCOC scheme requires an E_b/N_0 value of higher than 10 dB in order to perfectly converge. To summarize, EXIT chart results also somehow preferred the SECCC scheme over the others.

VI. CONCLUSION

We have devised near-capacity schemes based on iterative decoding for wireless communication. Comparison of the proposed channel coding schemes on account of the BER curves, as in Fig.11 reveals that the SECCC scheme outperforms the NCSCOC and CSCOC schemes, while setting the overall code rate equal in all the schemes. Likewise, EXIT chart visualization of the designed schemes reaffirms our claim that the SECCC strategy is greatly beneficial, as it offers fruitful convergence patterns for adaptation in future wireless communication systems. NCSCOC scheme never reaches its destiny of convergence. Though convergence is achieved in CSCOC scheme, but the BER curve of SECCC is significantly better than the CSCOC scheme. Conclusively, the SECCC system design is the best of all the proposed channel coding techniques in this exposition. More specifically, our experimental results show that the proposed CSCOC scheme with convergence capability outperforms its identical code rate counterpart NCSCOC scheme by about 3 dB at the PSNR degradation point of 1 dB. Additionally, an E_b/N_0 gain of 20 dB is attained using SECCC scheme capable to reach the point of perfect convergence, relative to identical code rate NCSCOC benchmarked scheme. Our future work would be the extension of the SECCC approach to be efficiently employed in Distributed SECCC (DSECCC) schemes, incorporating the concept of parallelism in SECCC scheme for profitable operation with less than or equal to 2048 number of bits and further invoking it in the multimedia streaming applications. In future, we are also interested to extend the application of SECCC approach using Unequal Error Protection (UEP) mechanism in the H.264/AVC standard multimedia streaming applications.

REFERENCES
[1] B. Vucetic and J. Yuan, *Space-Time Coding*. Hoboken, NJ, USA: Wiley, 2003.
[2] L. Hanzo, O. Alamri, M. El-Hajjar, and N. Wu, *Near-Capacity Multi-Functional MIMO Systems: Sphere-Packing, Iterative Detection and Cooperation*, vol. 4. Hoboken, NJ, USA: Wiley, 2009.

[3] A. Banerjee, K. Vaesen, A. Visweswaran, K. Khalaf, Q. Shi, S. Brebels, D. Guermandi, C.-H. Tsai, J. Nguyen, A. Medra, Y. Liu, G. Mangraviti, O. Furxhi, B. Gyselinckx, A. Bourdoux, J. Craninckx, and P. Wambacq, "Millimeter-wave transceivers for wireless communication, radar, and sensing," in *Proc. IEEE Custom Integr. Circuits Conf. (CICC)*, Apr. 2019, pp. 1–11.

[4] L. Hanzo, M. El-Hajjar, and O. Alamri, "Near-capacity wireless transceivers and cooperative communications in the MIMO era: Evolution of standards, waveform design, and future perspectives," *Proc. IEEE*, vol. 99, no. 8, pp. 1343–1385, Aug. 2011.

[5] P. Pathak and R. Bhatia. (Apr. 1, 2020). *Channel Coding for Wireless Communication Systems: A Review*. [Online]. Available: https://ssrn.com/abstract=3565791, doi: 10.2139/ssrn.3565791.

[6] C. E. Shannon, "A mathematical theory of communication," *Bell Syst. Tech. J.*, vol. 27, no. 3, pp. 379–423, Jul./Oct. 1948.

[7] Nasruminallah, M. El-Hajjar, N. S. Othman, A. P. Quang, and L. Hanzo, "Over-complete mapping aided, soft-bit assisted iterative unequal error protection H.264 joint source and channel decoding," in *Proc. IEEE 68th Veh. Technol. Conf.*, Sep. 2008, pp. 1–5.

[8] R. W. Hamming, "Error detecting and error correcting codes," *Bell Syst. Tech. J.*, vol. 29, no. 2, pp. 147–160, Apr. 1950.

[9] M. El-Hajjar and L. Hanzo, "EXIT charts for system design and analysis," *IEEE Commun. Surveys Tuts.*, vol. 16, no. 1, pp. 127–153, 1st Quart., 2014.

[10] M. F. U. Butt, "Self-concatenated coding for wireless communication systems," Ph.D. dissertation, School Electron. Comput. Sci., Univ. Southampton, Southampton, U.K., 2010.

[11] L. Hanzo, L.-L. Yang, E. Kuan, and K. Yen, *Single-and Multi-Carrier DS-CDMA: Multi-User Detection, Space-Time Spreading, Synchronisation, Standards and Networking*. Hoboken, NJ, USA: Wiley, 2003.

[12] L. Hanzo, T. H. Liew, and B. L. Yeap, *Turbo Coding, Turbo Equalisation, and Space-Time Coding*. Hoboken, NJ, USA: Wiley, 2002.

[13] L. Hanzo, S. X. Ng, W. Webb, and T. Keller, *Quadrature Amplitude Modulation: From Basics to Adaptive Trellis-Coded, Turbo-Equalised and Space-Time Coded OFDM, CDMA and MC-CDMA Systems*. Hoboken, NJ, USA: Wiley, 2004.

[14] X. Timoneda, S. Abadal, A. Franques, D. Manessis, J. Zhou, J. Torrellas, E. Alarcon, and A. Cabellos-Aparicio, "Engineer the channel and adapt to it: Enabling wireless intra-chip communication," *IEEE Trans. Commun.*, vol. 68, no. 5, pp. 3247–3258, May 2020.

[15] C. Berrou, A. Glavieux, and P. Thitimajshima, "Near Shannon limit error-correcting coding and decoding: Turbo-codes. 1," in *Proc. IEEE Int. Conf. Commun. (ICC)*, vol. 2, May 1993, pp. 1064–1070.

[16] C. Berrou and A. Glavieux, "Near optimum error correcting coding and decoding: Turbo-codes," *IEEE Trans. Commun.*, vol. 44, no. 10, pp. 1261–1271, Oct. 1996.

[17] G. D. Forney, *Concatenated Codes*. Cambridge, MA, USA: MIT Press, 1965.

[18] M. F. U. Butt, S. X. Ng, and L. Hanzo, "Self-concatenated code design and its application in power-efficient cooperative communications," *IEEE Commun. Surveys Tuts.*, vol. 14, no. 3, pp. 858–883, 3rd Quart., 2011.

[19] J. A. Ritcey, "Bit-interleaved coded modulation with iterative decoding using soft feedback," *Electron. Lett.*, vol. 34, no. 10, pp. 942–943, May 1998.

[20] X. Wang and H. V. Poor, "Iterative (turbo) soft interference cancellation and decoding for coded CDMA," *IEEE Trans. Commun.*, vol. 47, no. 7, pp. 1046–1061, Jul. 1999.

[21] A. Sezgin, D. Wubben, and V. Kuhn, "Analysis of mapping strategies for turbo-coded space-time block codes," in *Proc. IEEE Inf. Theory Workshop*, Mar./Apr. 2003, pp. 103–106.

[22] H. V. Nguyen, C. Xu, S. X. Ng, and L. Hanzo, "Near-capacity wireless system design principles," *IEEE Commun. Surveys Tuts.*, vol. 17, no. 4, pp. 1806–1833, 4th Quart., 2015.

[23] H. Chen, R. G. Maunder, and L. Hanzo, "A survey and tutorial on low-complexity turbo coding techniques and a holistic hybrid ARQ design example," *IEEE Commun. Surveys Tuts.*, vol. 15, no. 4, pp. 1546–1566, 4th Quart., 2013.

[24] P. Robertson and T. Worz, "Bandwidth-efficient turbo trellis-coded modulation using punctured component codes," *IEEE J. Sel. Areas Commun.*, vol. 16, no. 2, pp. 206–218, Feb. 1998.

[25] D. Divsalar and F. Pollara, "Multiple turbo codes for deep-space communications," TDA Progr. Rep. vol. 42-121, May 1995, pp. 66–77.

[26] S. Benedetto and G. Montorsi, "Serial concatenation of block and convolutional codes," *Electron. Lett.*, vol. 32, no. 10, pp. 887–888, May 1996.

[27] P. Elias, "Coding for noisy channels," *IRE Conv. Rec*, vol. 3, no. 4, pp. 37–46, 1955.

[28] J. M. Wozencraft, "Sequential decoding for reliable communication," in *Proc. IRE Nat. Conv. Rec.*, vol. 5, pt. 2, 1957, pp. 11–25.

[29] J. M. Wozencraft and B. Reiffen, *Sequential Decoding*, vol. 10. Cambridge, MA, USA: MIT Press, 1961.

[30] R. Fano, "A heuristic discussion of probabilistic decoding," *IEEE Trans. Inf. Theory*, vol. IT-9, no. 2, pp. 64–74, Apr. 1963.

[31] J. Massey, *Threshold Decoding*. Cambridge, MA, USA: MIT Press, 1963.

[32] A. Viterbi, "Error bounds for convolutional codes and an asymptotically optimum decoding algorithm," *IEEE Trans. Inf. Theory*, vol. IT-13, no. 2, pp. 260–269, Apr. 1967.

[33] G. D. Forney, Jr., "The Viterbi algorithm," *Proc. IEEE*, vol. 61, no. 3, pp. 268–278, Mar. 1973.

[34] L. Bahl, J. Cocke, F. Jelinek, and J. Raviv, "Optimal decoding of linear codes for minimizing symbol error rate (Corresp.)," *IEEE Trans. Inf. Theory*, vol. IT-20, no. 2, pp. 284–287, Mar. 1974.

[35] F. I. Alajaji and N. C. Phamdo, "Soft-decision COVQ for Rayleigh-fading channels," *IEEE Commun. Lett.*, vol. 2, no. 6, pp. 162–164, Jun. 1998.

[36] J. Jiang and K. R. Narayanan, "Iterative soft decision decoding of Reed Solomon codes based on adaptive parity check matrices," in *Proc. Int. Symp. Inf. Theory (ISIT)*, Jun./Jul. 2004, p. 261.

[37] G. Jeong and D. Hsia, "Optimal quantization for soft-decision turbo decoder," in *Proc. Gateway 21st Century Commun. Village. VTC-Fall. IEEE VTS 50th Veh. Technol. Conf.*, vol. 3, Sep. 1999, pp. 1620–1624.

[38] S. Bhattacharjee, M. Damrath, and P. A. Hoeher, "EXIT chart analysis of higher order modulation schemes in molecular communications," in *Proc. 6th Annu. ACM Int. Conf. Nanosc. Comput. Commun.*, Sep. 2019, pp. 1–6.

[39] J. Hagenauer, "The turbo principle: Tutorial introduction and state of the art," in *Proc. Int. Symp. Turbo Codes Rel. Topics*, 1997, pp. 1–11.

[40] S. Benedetto, D. Divsalar, G. Montorsi, and F. Pollara, "Serial concatenation of interleaved codes: Performance analysis, design, and iterative decoding," *IEEE Trans. Inf. Theory*, vol. 44, no. 3, pp. 909–926, May 1998.

[41] S. Benedetto, D. Divsalar, G. Montorsi, and F. Pollara, "Analysis, design, and iterative decoding of double serially concatenated codes with interleavers," *IEEE J. Sel. Areas Commun.*, vol. 16, no. 2, pp. 231–244, Feb. 1998.

[42] N. Nasruminallah and L. Hanzo, "Near-capacity H.264 multimedia communications using iterative joint source-channel decoding," *IEEE Commun. Surveys Tuts.*, vol. 14, no. 2, pp. 538–564, 2nd Quart., 2012.

[43] J. Kliewer, N. Goertz, and A. Mertins, "Iterative source-channel decoding with Markov random field source models," *IEEE Trans. Signal Process.*, vol. 54, no. 10, pp. 3688–3701, Oct. 2006.

[44] S. Xin Ng, M. F. U. Butt, and L. Hanzo, "On the union bounds of self-concatenated convolutional codes," *IEEE Signal Process. Lett.*, vol. 16, no. 9, pp. 754–757, Sep. 2009.

[45] H. Kalva, "The H.264 video coding standard," *IEEE MultimediaMag.*, vol. 13, no. 4, pp. 86–90, Oct./Dec. 2006.

[46] G. J. Sullivan, J. M. Boyce, Y. Chen, J.-R. Ohm, C. A. Segall, and A. Vetro, "Standardized extensions of high efficiency video coding (HEVC)," *IEEE J. Sel. Topics Signal Process.*, vol. 7, no. 6, pp. 1001–1016, Dec. 2013.

[47] R. Maunder, J. Kliewer, S. Ng, J. Wang, L.-L. Yang, and L. Hanzo, "Joint iterative decoding of trellis-based VQ and TCM," *IEEE Trans. Wireless Commun.*, vol. 6, no. 4, pp. 1327–1336, Apr. 2007.

[48] D. Divsalar, S. Dolinar, and F. Pollara, "Low complexity turbo-like codes," in *Proc. 2nd Int. Symp. Turbo Codes*, Sep. 2000, pp. 73–80.

[49] S. ten Brink, "Convergence behavior of iteratively decoded parallel concatenated codes," *IEEE Trans. Commun.*, vol. 49, no. 10, pp. 1727–1737, Oct. 2001.

[50] M. Tüchler, S. Ten Brink, and J. Hagenauer, "Measures for tracing convergence of iterative decoding algorithms," in *Proc. 4th IEEE/ITG Conf. Source Channel Coding*, 2002, pp. 50–63.

[51] F. Brannstrom, L. K. Rasmussen, and A. J. Grant, "Convergence analysis and optimal scheduling for multiple concatenated codes," *IEEE Trans. Inf. Theory*, vol. 51, no. 9, pp. 3354–3364, Sep. 2005.

[52] S. Ten-Brink, "Designing iterative decoding schemes with the extrinsic information transfer chart," *AEU Int. J. Electron. Commun.*, vol. 54, no. 6, pp. 389–398, 2000.

[53] N. Zheng, Y. He, B. Bai, A. M.-C. So, and K. Yang, "LDPC code design for Gaussian multiple-access channels using dynamic EXIT chart analysis," in *Proc. IEEE Int. Conf. Acoust., Speech Signal Process. (ICASSP)*, Mar. 2017, pp. 3679–3683.

[54] F. Cheng, A. Liu, Q. Zhang, Y. Zhang, and B. Cai, "Codes design based on EXIT chart for polar coded BICM-ID," in *Proc. IEEE 2nd Adv. Inf. Technol., Electron. Autom. Control Conf. (IAEAC)*, Mar. 2017, pp. 1129–1133.

[55] M. Damrath, M. Schurwanz, and P. A. Hoeher, "The turbo principle in molecular communications," in *Proc. 12th Int. ITG Conf. Syst., Commun. Coding (SCC)* Frankfurt, Germany: VDE, 2019, pp. 1–6.

[56] P. M. Shah, P. D. Vyavahare, and A. Jain, "Performance analysis of turbo iterative decoder with EXIT chart," in *Proc. Recent Adv. Interdiscipl. Trends Eng. Appl.*, Apr. 2019, pp. 1–4.

[57] I. Granada, P. M. Crespo, and J. Garcia-Frías, "Asymptotic BER EXIT chart analysis for high rate codes based on the parallel concatenation of analog RCM and digital LDGM codes," *EURASIP J. Wireless Commun. Netw.*, vol. 2019, no. 1, p. 11, Dec. 2019.

[58] M. F. U. Butt, R. A. Riaz, S. X. Ng, and L. Hanzo, "Near-capacity iteratively decoded binary self-concatenated code design using EXIT charts," in *Proc. IEEE Global Telecommun. Conf. (GLOBECOM)*, Nov. 2008, pp. 1–5.

[59] J. Korhonen and J. You, "Peak signal-to-noise ratio revisited: Is simple beautiful?" in *Proc. 4th Int. Workshop Qual. Multimedia Exper.*, Jul. 2012, pp. 37–38.

[60] K. Li and X. Wang, "EXIT chart analysis of turbo multiuser detection," *IEEE Trans. Wireless Commun.*, vol. 4, no. 1, pp. 300–311, Jan. 2005.

NASRU MINALLAH received the B.Sc. degree in computer engineering from the University of Engineering and Technology, Peshawar, Pakistan, in 2004, the M.Sc. degree in computer engineering from the Lahore University of Management Sciences, Lahore, Pakistan, in 2006, and the Ph.D. degree from the Communications Group, School of Electronics and Computer Science, University of Southampton, Southampton, U.K., in 2010. He is currently working as an Associate Professor with the Department of Computer Systems Engineering, University of Engineering and Technology Peshawar. His research interests include image processing, remote sensing, and low-bit-rate video coding for wireless communications.

MUHAMMAD FASIH UDDIN BUTT (Member, IEEE) received the B.E. degree from the National University of Sciences and Technology (NUST), Pakistan, in 1999, the M.E. degree from the Center for Advanced Studies in Engineering, UET Taxila, Pakistan, with specialization in digital communication/computer networks, in 2003, and the Ph.D. degree in electronics and electrical engineering from the School of Electronics and Computer Science, University of Southampton, U.K., in June 2010. He is currently an Associate Professor and the Head of the Next Generations Communications Research Group, Department of Electrical Engineering, COMSATS University Islamabad, Pakistan, where he has been serving as an Academician, since 2002. He has published over 30 research papers in various reputed journals and conference proceedings. His research interests include channel coding, cooperative cognitive radio networks, mm wave radio-over-fiber technologies, physical layer security, and cyber security.

IMRAN ULLAH KHAN (Member, IEEE) received the bachelor's degree in electronic engineering from the NED University of Engineering and Technology, Karachi, Pakistan, in 2002, the M.Sc. degree in electrical engineering from the University of Engineering and Technology Peshawar, Pakistan, in 2008, and the Ph.D. degree in communication networks from University Malaysia Sarawak (UNIMAS), Malaysia, in 2014. He was with the Department of Electrical Engineering, Federal Urdu University of Arts, Science, and Technology, Islamabad Pakistan, from April 2005 to March 2015. He has been Head of Department (HOD) and an Assistant Professor/Associate Professor with the Electrical Engineering Department, Qurtuba University of Science and Information Technology, from July 2015 to August 2018. He has been working as a Professor with the College of Underwater Acoustics Engineering, Harbin Engineering University, China, since September 2018. He has supervised many research projects at undergraduate and graduate levels. He has authored many journal papers (SCIE and ESCI) and conferences papers. His research interests include physical and MAC layers-based cooperative diversity wireless communications protocols, underwater cooperative diversity protocols, and half duplex and full duplex underwater communication protocols. He is a member of the Pakistan Engineering Counsel (PEC). He is also a Technical Member of the National Curriculum Review Committee (NCRC) Higher Education Commission (HEC), Pakistan, the Academic Counsel (AC), and Board of Study (BOS) Committee Qurtuba University of Science and IT. He also received research grants from HEC Pakistan and Higher Education Malaysia. He has also been serving as a Designated Reviewer for many reputed international journals.

ISHTIAQUE AHMED received the B.Sc. degree in electrical engineering, with specialization in telecommunication, from COMSATS University Islamabad, Pakistan, in 2018. He is currently serving as a Research Assistant with the National Center of Big Data and Cloud Computing, University of Engineering and Technology Peshawar (NCBC-UETP) Pakistan. His research interests include wireless communication, channel coding, low-bit-rate video encoding, multimedia streaming, distributed generation, and smart grids management and privacy.

KHURRAM S. KHATTAK received the Ph.D. degree from The George Washington University, DC, USA, in 2017. He is currently working as an Assistant Professor with the Department of Computer Systems Engineering, University of Engineering and Technology Peshawar. His research interests include intelligent transportation systems, the Internet of Things (IoT), and embedded systems.

GANG QIAO (Member, IEEE) received the bachelor's, master's, and Ph.D. degrees from the College of Underwater Acoustic Engineering, Harbin Engineering University, China, in 1996, 1999, and 2004, respectively. Since 1999, he has been with the College of Underwater Acoustic Engineering, Harbin Engineering University, where he is currently a Professor and the Associate Dean. He has already published more than 80 articles. He holds seven national invention patents. His current research interests include underwater communication and networks, detection and positioning of underwater targets, and the sonar designed for small carriers. He is a member of the Acoustical Society of China and the Youth Federation of Heilongjiang Province. He has received the National Award for the Outstanding Scientific and Technological Workers and the Science and Technology Award for Young Talents in Heilongjiang. He is the Vice Chairman of the Robotics Society of Heilongjiang Province.
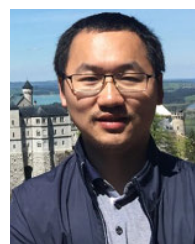
SONGZUO LIU (Member, IEEE) received the B.S. and Ph.D. degrees in signal and information processing from Harbin Engineering University (HEU), Harbin, China, in 2008 and 2014, respectively. He has been an Associate Professor with the College of Underwater Acoustic Engineering, HEU, since 2017. His research interests include covert and biologically inspired underwater acoustic communication, underwater acoustic communication and networking, and design and implementation of underwater acoustic modem.

• • •